

PACS numbers: 42.55.Wd; 42.60.By; 42.65.Re; 42.60.Jf
DOI: 10.1070/QE2013v043n03ABEH015132

Hybrid Er/Yb fibre laser system for generating few-cycle 1.6 to 2.0 μm pulses optically synchronised with high-power pulses near 1 μm

A.V. Andrianov, E.A. Anashkina, S.V. Muravyev, A.V. Kim

Abstract. **This paper presents the concept of fibre laser system design for generating optically synchronised femtosecond pulses at two, greatly differing wavelengths and reports experimental and numerical simulation studies of nonlinear conversion of femtosecond pulses at 1.5 μm wavelength in a dispersion-shifted fibre, with the generation of synchronised pulses in the ranges 1.6–2 and 1–1.1 μm. We describe a three-stage high-power fibre amplifier of femtosecond pulses at 1 μm and a hybrid Er/Yb fibre laser system that has enabled the generation of 12 fs pulses with a centre wavelength of 1.7 μm, synchronised with high-power (microjoule level) 250 fs pulses at 1.03 μm.**

Keywords: *few-cycle optical pulses, optical synchronisation of femtosecond pulses, nonlinear fibre optics, femtosecond fibre lasers and amplifiers.*

1. Introduction

One important issue in modern laser physics is the development of ultrashort (femtosecond and subpicosecond) pulse laser sources with high pulse energy, peak intensity and average power. Such sources are needed primarily for scientific applications. In addition, recent years have seen increasing interest in such sources for laser machining of materials (including micro- and nanostructured materials) and biomedical applications. In this context, fibre laser sources – which take full advantage of the well-established fibre-optic solutions employed in telecom systems – hold considerable promise. Moreover, fibre laser systems can outperform solid-state lasers in average power due to optimal amplification conditions in the active fibres, which enable efficient pumping by high-power laser diodes and efficient heat removal.

Fibre systems are also of great interest for generating optically synchronised coherent femtosecond pulses differing greatly in wavelength. Such pulses are needed primarily for parametric amplifiers of ultrashort pulses (USPs), where the pump and signal waves should be exactly synchronised. The many high-power femtosecond parametric systems demonstrated to date employ electronic synchronisation [1–5], which requires careful adjustment and is a potential instability source. In recent years, there has been considerable interest in optical synchronisation systems [6]. In particular, Andriukaitis et al. [7] and Teisset et al. [8] obtained pump and signal pulses using different spectral components of a supercontinuum generated in a bulk element and photonic crystal fibres.

In this paper, we report the generation of femtosecond pulses by an erbium-doped fibre laser in the 1.5 μm range, followed by nonlinear optical conversion in a dispersion-shifted silica fibre for obtaining synchronised pulses in the ranges 1.6–2 and 1.0–1.1 μm [9] and further increase in the energy of the shorter wavelength pulse in a multistage all-fibre ytterbium-doped amplifier. Such a system allows one to obtain, on the one hand, high-power pulses near 1 μm and, on the other, optically synchronised pulses differing greatly in wavelength, with the possibility of minimising the duration of the pulse in the range 1.6–2 μm [10].

It should be noted that the generation of USPs at wavelengths near 1 μm by fibre lasers is a challenging problem. Conventional USP generation in such lasers in the mode-locking regime is impeded by the lack of fibres with anomalous dispersion in the 1 μm range. One known approach to pulse generation in fibre lasers is based on the use of a semiconductor saturable absorber mirror (SESAM), which should be matched to the fibre cavity in a special way [11]. The necessity to match this component to the fibre scheme and its limited service time are drawbacks to this approach. Another approach to pulse generation in fibre lasers is based on mode locking in a laser with a normal net dispersion [12]. This configuration, however, is not all-fibre either: it contains fibre to free couplers and intracavity bulk optical components, which impair the stability of the system to external influences.

Fermann et al. [13] proposed a scheme in which 1.5 μm pulses generated by an erbium-doped fibre laser were converted to the 1 μm range. In this scheme, the shorter wavelength pulses result from Raman conversion of the input wavelength (1.5 μm) to the 2 μm range in a nonlinear fibre, followed by frequency doubling through second harmonic generation in a periodically poled lithium niobate crystal. The necessity to use such a crystal, a bulk optical component, is a drawback to this scheme: it cannot be made all-fibre.

Kieu et al. [14] demonstrated partial optical energy conversion from 1.5 to 1 μm wavelength in a fibre-optic system in an optical supercontinuum generation process. The erbium-doped fibre laser oscillator used (1.5 μm) was mode-locked using carbon nanotubes. The signal was converted to 1 μm wavelength in a highly nonlinear fibre and then chirped, amplified in an ytterbium-doped fibre and compressed with a grating compressor. The system has the drawback of using

A.V. Andrianov, E.A. Anashkina, S.V. Muravyev, A.V. Kim Institute of Applied Physics, Russian Academy of Sciences, ul. Ul'yanova 46, 603950 Nizhnii Novgorod, Russia;
e-mail: alex.v.andrianov@gmail.com, elena.anashkina@gmail.com, mur@ufp.appl.sci-nnov.ru, kim@ufp.appl.sci-nnov.ru

Received 24 December 2012
Kvantovaya Elektronika **43** (3) 256–262 (2013)
Translated by O.M. Tsarev

supercontinuum generation, which leads to a low degree of conversion from 1.5 to 1 μm wavelength.

2. Concept and design of a synchronised two-frequency source

The concept of the proposed laser system is based on the use of a scheme comprising an all-fibre femtosecond seed source, 1.57 μm preamplifier, nonlinear fibre-optic wavelength converter to the 1 μm range and diode-pumped three-stage fibre-optic amplifier. The configuration of the laser system is shown in Fig. 1. The master oscillator used (λ = 1.57 μm) was a diode-pumped all-fibre erbium-doped femtosecond ring laser. The laser was passively mode-locked using nonlinear rotation of the polarisation ellipse of a femtosecond pulse due to the optical Kerr effect. The seed laser generated 230 fs pulses at a repetition rate of 49 MHz. The pulses were amplified by an erbium-doped fibre amplifier and compressed to ~70 fs duration in a nonlinear optical fibre compressor.

One distinctive feature of the laser system was the use of a nonlinear fibre-optic femtosecond-pulse wavelength converter from the 1.5 μm range to 1 μm. This conversion allowed us to obtain femtosecond pulses at wavelengths in the range 1–1.1 μm, which were then amplified with high efficiency by ytterbium-doped fibres. The nonlinear optical converter used was a short piece (shorter than 10 cm) of dispersion-shifted fibre (DSF) with a zero-dispersion point at 1.4 μm. At the input pulse wavelength, the second-order dispersion in this fibre was $\beta_2 = -8$ ps^2 km^{-1}. A portion of the initial pulse energy was converted to an about 1 μm wavelength through spectral broadening upon soliton compression in the low anomalous dispersion region and linear wave generation in the normal dispersion region under phase-matching conditions.

The pulses ($\lambda \approx 1$ μm) were further amplified in an all-fibre three-stage amplifier. To obtain a high output pulse energy and minimise nonlinear effects in the active fibres, stretched chirped pulses were amplified and the pulse repetition rate was reduced with the aim of lowering the required average pump power. Because of this, after the nonlinear converter the 1 μm pulses were stretched to ~100 ps duration in a stretcher fibre. Next, the chirped pulses were amplified in the first stage of the ytterbium-doped fibre amplifier in order to compensate for the energy loss due to the nonlinear conversion.

The next component of the system was an acousto-optic modulator (AOM) for reducing the pulse repetition rate. The control circuit of the AOM was such that it transmitted every Nth pulse (N was set electronically in the range 1 to 64). The decimated sequence was amplified in the second stage of the ytterbium-doped fibre amplifier. The pulse energy and average power were raised further in the final amplifier stage, made of a double-clad specialty active fibre with a large core size (25 μm). This fibre was pumped by 6-W multimode laser diodes, which allowed us to reach an output pulse power of 1.2 W at a 1 MHz pulse repetition rate and significant nonlinear distortions of the spectrum, and 0.9 W at weaker nonlinear distortions. The pulses were then compressed to 250 fs duration using a reflective diffraction grating.

3. Experimental study and numerical simulation of two-frequency signal generation in DSF

The proposed method for generating few-cycle pulses in the range 1.6–2 μm with optically synchronised pulses in the range 1–1.1 μm builds on the concept of dispersive wave emission during high-order soliton compression of an input pulse propagating through a DSF. It should be noted that, in foreign publications, dispersive waves are often referred to as Cherenkov radiation, which reflects the fact that an emitted high-frequency pulse is synchronous with the soliton that has emitted it [15, 16]. Earlier, we demonstrated the possibility of obtaining few-cycle pulses through high-order soliton compression [10] and the generation of dispersive waves [9]. In this study, major attention is focused on the possibility of simultaneous, synchronised generation of a few-cycle pulse and a high-frequency dispersive wave pulse.

In our experiments, pulses from the output of the erbium-doped fibre amplifier (~70 fs duration, 2 nJ energy) propagated through a piece of DSF. The fibre length was adjusted experimentally by gradually reducing it. In addition, the diode pump power coupled into the amplifier and, accordingly, the pulse energy at the DSF input were varied in a narrow range (±10%). The broadband signal at the DSF output was analysed using a scanning monochromator spectrometer. The pulse shape was evaluated using frequency-resolved optical gating (FROG) [17].

Parameters of the system were optimised by numerical simulation using realistic input-pulse and DSF parameters. The spectral and temporal evolution of femtosecond pulses was analysed theoretically in terms of a one-way wave equation [10, 18] using the pseudospectral, split-step Fourier method (SSFM) [19]. This approach allows one to take into account the combined effect of an arbitrary dispersion profile and Kerr nonlinearity due to both the essentially instantaneous electronic response and delayed molecular response of the medium. Figure 2 presents numerical simulation results illustrating the evolution of the spectrum and temporal pro-

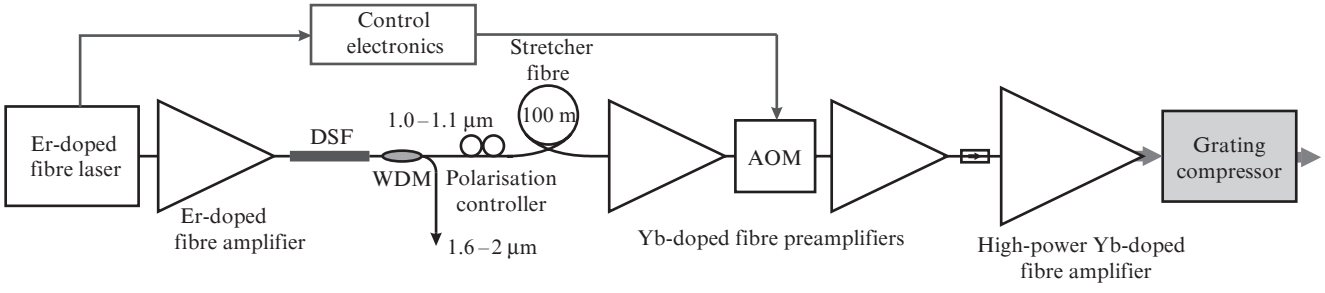

Figure 1. Configuration of the fibre laser system.

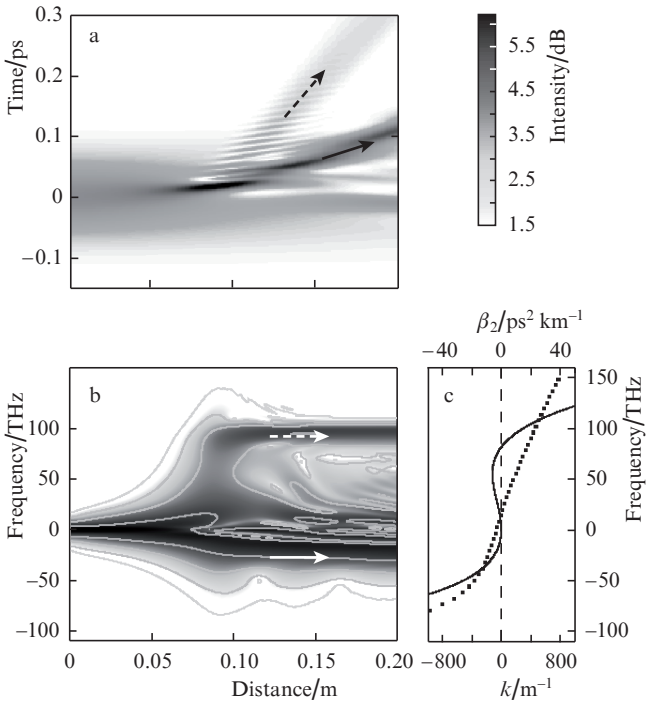

Figure 2. Numerical simulation of pulse propagation in a DSF: (a) evolution of the intensity distribution, (b) evolution of the spectrum. The solid and dotted lines represent, respectively, the propagation constant k and second-order dispersion coefficient β_2 in the fibre. The solid and dashed lines in panel (c) represent the positions of the soliton and short-wavelength pulse of dispersive waves, respectively.

file of a pulse propagating through the DSF. Also shown in Fig. 2 are the second-order dispersion coefficient of the fibre and the propagation constant in the fibre in the frame of reference where the input pulse is at rest.

The numerical simulation results demonstrate that, in the first step of propagation through the nonlinear fibre, the pulse experiences compression and the corresponding spectral broadening, which is attributable to high-order soliton compression in the initial stage of continuum generation in the anomalous dispersion regime. Before the onset of high-order soliton fission [18], the spectrum broadens to the extent that an appreciable part of its high-frequency wing falls in the normal dispersion region and can act as a source of linear dispersive waves. The emission of linear dispersive waves by a soliton pulse to the normal dispersion region in optical fibres was studied both theoretically and experimentally [15, 16] with application to fundamental and higher order solitons in silica and photonic-crystal fibres [20, 21] and to few-cycle pulses [22]. The dynamics of the high-frequency wing of the spectrum, which extends to the normal dispersion region, are dominated by those of a soliton pulse that forms in the anomalous dispersion region, so that the variations in the phases of all the high-frequency spectral components are coordinated, and their wavenumber is determined by that of the soliton [23]. When the phase matching condition is satisfied [15, 16, 21], dispersive waves are emitted most efficiently, resulting in a smooth spectral peak in the short-wavelength region. Efficient light transfer to the short-wavelength region takes place only within a small portion of the propagation path, where the soliton is most compressed and the spectrum has the largest width. Subsequently, the short-wavelength and soliton pulses diverge because of the difference in group velocity, which is well illustrated by the evolution of the intensity distribution in Fig. 2.

Two important features of the above process are worth noting: first, dispersive wave emission and maximum pulse compression occur synchronously and, second, dispersive wave radiation is coherent with the main soliton pulse. Thus, optically synchronised femtosecond pulses differing greatly in wavelength can be obtained in an all-fibre scheme based on a piece of DSF.

It is worth noting that, even though the maximum soliton compression occurs at a certain fibre length, dependent on input pulse parameters, the pulse duration remains short in a rather broad range of fibre lengths. In particular, in Fig. 2 the pulse has the shortest duration, 11 fs, at z = 9 cm, and its duration is less than 15 fs at z between 7 and 15 cm. For the purpose of this study, the optimal fibre length is that at which a pulse passes the largest compression point but experiences no excessive broadening, and the interaction with the short-wavelength radiation almost ceases.

In our experiments, the fibre length and input pulse energy were such that the observed spectral shape was most similar to the optimal shape inferred from numerical simulation results. In addition, the pulse shape was evaluated by the FROG technique. Figure 3 shows the simulated signal spectrum at the DSF output, and Fig. 4 presents the temporal intensity profiles retrieved from a measured FROG trace (Fig. 4, inset) and obtained by numerical simulation. The estimated FWHM pulse duration is 12 fs, i.e. two optical cycles. The trailing edge of the pulse has well-defined oscillations, attributable to the interference of the compressed higher order soliton with dispersive waves. The dotted line in Fig. 3 represents the spectrum of the high-frequency signal after filtration, and the solid curve above the shaded area represents the spectrum of the remaining, few-cycle pulse. Figure 4 shows the time-domain position of the corresponding pulses after filtration. The salient feature of the temporal intensity profile of the long-wavelength pulse in Fig. 4 is a sharp, strong peak over a broad pedestal, characteristic of high-order soliton compression. The duration of the short-wavelength pulse after filtration is 45 fs. It is worth noting that the simulation results agree very well with experimental data. The above

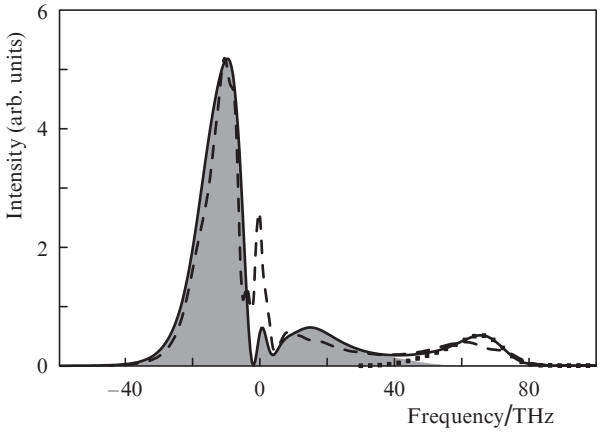

Figure 3. Measured and simulated spectra of the signal at the DSF output (dashed and solid lines, respectively) and low- and high-frequency pulse components filtered off in numerical simulation (solid curve above the shaded area and dotted line, respectively). Zero on the frequency axis corresponds to a wavelength of 1.5 μm.

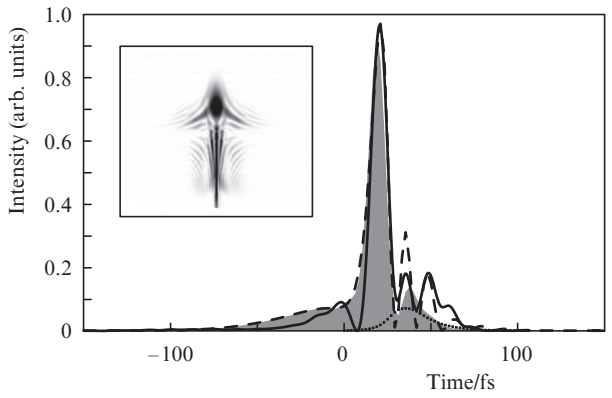

Figure 4. Signal intensity profile at the DSF output: numerical simulation (solid line), FROG-retrieved profile (dashed line) and low- and high-frequency pulse components filtered off in numerical simulation (solid curve above the shaded area and dotted line, respectively). Inset: measured FROG trace.

numerical simulation and experimental study demonstrate that two pulses differing greatly in centre wavelength can be optically synchronised in a DSF.

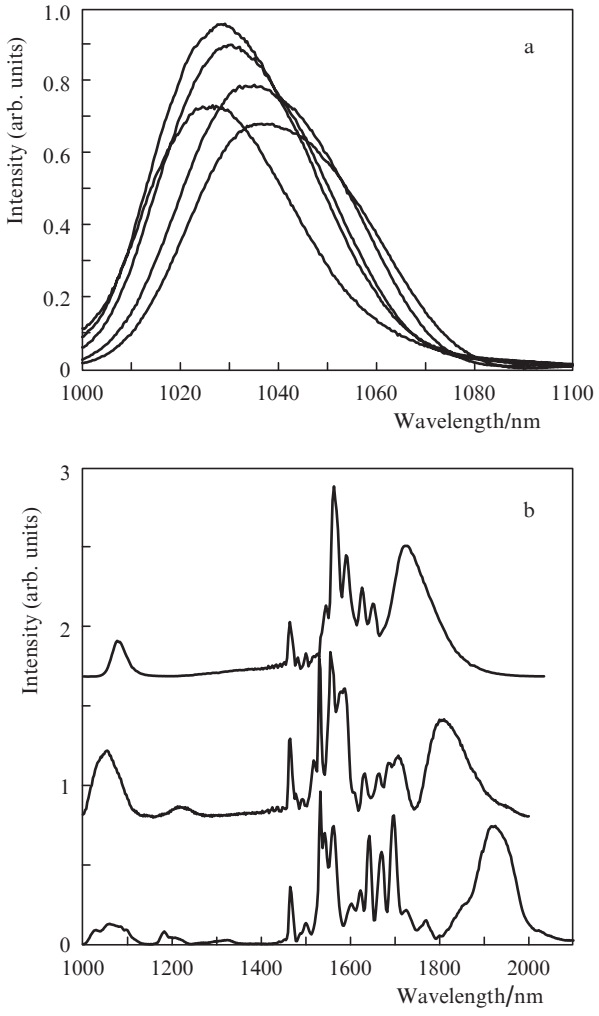

Figure 5. Tuning of the centre wavelength of the (a) short- and (b) long-wavelength pulses.

The wavelength of both the high- and low-frequency pulses can be tuned in a narrow range by varying the input pulse power ($\lambda = 1.5$ μm) and in a considerably wider range by using DSFs with different zero-dispersion wavelengths. Figure 5 illustrates the tuning of the centre wavelength of the low-frequency pulse and that of the high-frequency pulse after filtration in our experiments.

In our experimental setup, a WDM fibre coupler, intended to separate the short- and long-wavelength spectral regions, was fusion-spliced directly to the DSF output. Clearly, the dispersion of the fibres in the coupler will broaden pulses, but the controlled phase shift can be subsequently compensated in an appropriate compressor.

4. Amplification of 1-μm USPs: numerical simulation and experiment

In accordance with the general concept of high-power laser system design, the 1-μm signal energy was increased through chirped pulse amplification (CPA). A stretcher made of a polarisation-maintaining (PM) fibre was fusion-spliced behind the WDM coupler and polarisation controller. The first stage of the ytterbium-doped PM fibre amplifier, pumped by a single-mode laser diode, increased the pulse power from 1.5 to 220 mW (with an increase in pulse energy to 4 nJ). The measured bandwidth of the signal centred at 1030 nm was 21 nm.

The next component of the system was a PM fibre pigtailed AOM, intended to reduce the pulse repetition rate. In addition, owing to its short switch-on time (~10 ns) the AOM suppressed the amplified spontaneous emission from the first amplifier, thereby improving the contrast. The energy loss of the pulses in the AOM was ~50%, and the average power at the AOM output was 2 to 9 mW at pulse repetition rates from 1 to 4.5 MHz. The second amplifier stage was identical to the first and allowed the average pulse power to be increased to 90–150 mW. At a single-mode diode pump power of 250 mW, the signal power at the output of the second amplifier stage was 90 mW, which corresponded to a pulse energy of 90 nJ at a pulse repetition rate of 1 MHz. The pulse bandwidth was 20 nm. Further raising the pump power led to severe nonlinear distortions in the preamplifier. After the second stage, the signal arrived (through a Faraday isolator) at the output amplifier stage, made from a large mode area fibre. The pulse power at the amplifier output ranged up to 1.2 W. Nonlinear distortions of the spectrum were significant starting at a multimode pump power of 6 W. The nonlinear distortions can be minimised by reducing the output power to 0.9 W and optimising the stretcher fibre length.

To find the optimal stretcher length, we performed numerical simulation of the amplification process in the three-stage amplifier. The transform-limited 70 fs input signal was taken to have a Gaussian spectrum with a centre wavelength of 1.03 μm. The pulse energy was 50–100 nJ after the second amplifier stage and ~1 μJ after the output stage. The ytterbium-doped active fibre in the final stage was 3 m long and had a core diameter of 25 μm and numerical aperture of 0.06. The signal was assumed to be amplified in the single-mode regime. By fitting the fundamental mode field distribution with a Gaussian, the nonlinearity coefficient was determined to be $\gamma = 0.5$ W^{-1} km^{-1}. The shape of the gain band was calculated using previous data [24]. The model took into account the Kerr and Raman nonlinearities and dispersion in the fibre.

To minimise the distortions induced by the Kerr and Raman nonlinearities, the pulse to be amplified was assumed to be stretched (chirped). The stretcher used was Nufern PM 980 normal dispersion fibre, with second- and third-order dispersion coefficients $\beta_2 = 50$ ps^2 km^{-1} and $\beta_3 = 0.05$ ps^3 km^{-1}. After amplification in the ytterbium-doped fibre amplifier, the pulses were compressed in a grating compressor with a negative second-order dispersion and positive third-order dispersion [25]. The physical picture of the amplification process suggests that a long stretcher is undesirable because, after compression in the grating compressor, there remains an uncompensated cubic phase, which leads to pulse stretching and pedestal formation. In view of this, the stretcher length was optimised using numerical simulation. Since the gain band of the ytterbium-doped fibre is narrower than the spectrum of the input signal, amplification in the active fibre will be accompanied by spectral narrowing. Basically, the final spectrum is determined by the shape of the gain band, as was demonstrated by numerical simulation. At a low degree of pulse stretching, pulse propagation in the active fibre is substantially nonlinear.

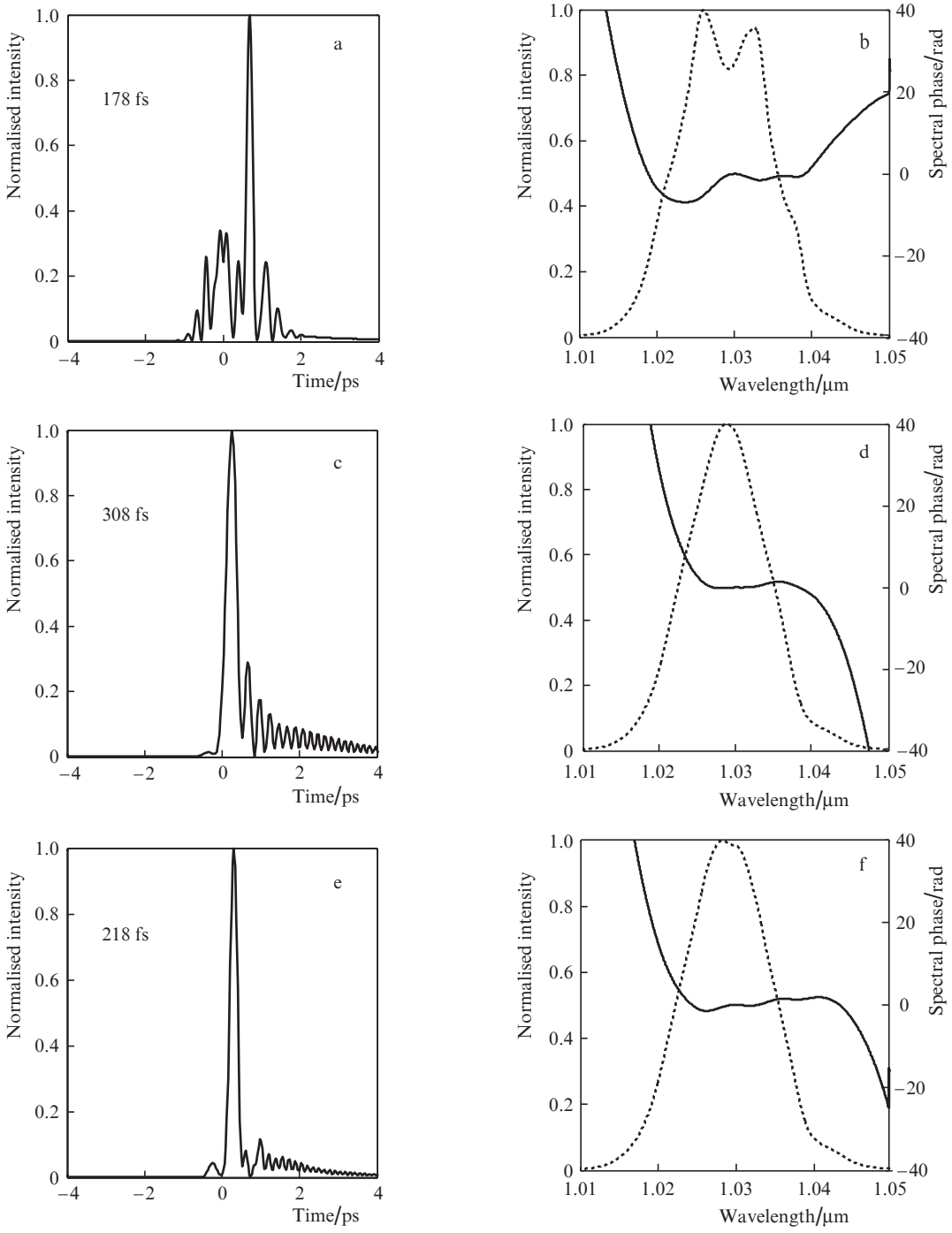

Figure 6. (a, c, e) Intensity profiles of amplified pulses after compression and (b, d, f) spectrum (dotted line) and spectral phase (solid line) of compressed pulses at stretcher lengths of (a, b) 50, (c, d) 150 and (e, f) 100 m.

Figure 6 presents numerical simulation results for stretcher lengths of 50, 150 and 100 m. At a stretcher length of 50 m (Fig. 6a), the maximum peak power in the amplifier reaches the level where the effect of self-phase modulation is significant and the pulse acquires a large nonlinear phase, which leads to severe distortions of its spectrum. The central peak of the pulse can be compressed to ~180 fs in the compressor, but the large pedestal with a complex structure is undesirable. The calculated spectrum and spectral phase after compression are shown in Fig. 6b. At a stretcher length of 150 m, the nonlinear phase shift is rather small, but the large third-order dispersion in both the fibre and grating compressor makes it impossible to compress the pulse to near the transform limit (120 fs in the case under consideration) and leads to oscillations on the trailing edge of the pulse (Fig. 6c). The calculated spectrum and spectral phase after compression are shown in Fig. 6d.

According to numerical simulation results, the optimal stretcher length is ~100 m. In this case, the nonlinear phase shift in the amplifier is less significant than that at a stretcher length of 50 m and the effect of third-order dispersion is weaker than that with the 150-m stretcher. In addition, the pulse duration after compression is ~220 fs, and the pedestal accounts for the smallest fraction of the energy (Fig. 6e). The spectrum and spectral phase after compression for the optimal parameters are presented in Fig. 6f.

Figure 7 shows the experimental spectrum obtained when the maximum power of the output amplifier was 0.9 W. The pulses were compressed using one gold-coated reflective diffraction grating (1200 lines mm^{-1}). The signal power at the compressor output was 0.6 W. Thus, the efficiency was about 70%. The compressor was adjusted to the minimum autocorrelation pulse width.

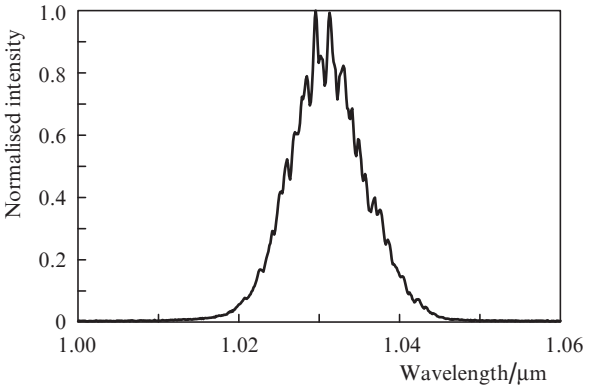

Figure 7. Spectrum of a pulse amplified by the ytterbium-doped fibre amplifiers.

Figure 8 presents pulse intensity and phase profiles retrieved from FROG measurements. The FWHM pulse duration is 250 fs, in agreement with autocorrelation measurements. It is seen that the phase shift is incompletely compensated by the compressor, as also evidenced by the pulse time–bandwidth product of 0.7. The distinction from the transform limit is caused by the uncompensated third-order dispersion and nonlinear phase distortions.

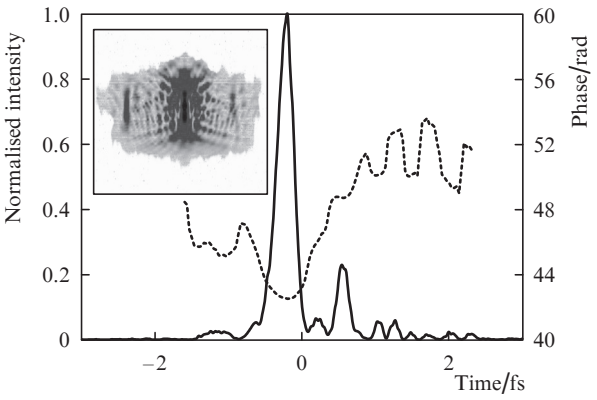

Figure 8. FROG-retrieved pulse intensity (solid line) and phase (dashed line) profiles at the grating compressor output. Inset: measured FROG trace.

5. Conclusions

We have developed a compact fibre laser system that generates optically synchronised few-cycle pulses at wavelengths of 1.0–1.1 and 1.6–2 μm. The minimum duration of the longer wavelength pulses is 12 fs, i.e. two optical cycles. We have demonstrated amplification of few-cycle pulses in a high-power fibre amplifier to microjoule energies and compression of the pulses in a grating compressor to 250 fs duration. The laser system can be used as a source of synchronised pulses for further amplification by parametric and laser amplifiers and also in biomedical studies, micromodification of materials, terahertz generation and pump–probe experiments.

Acknowledgements. This work was supported by the Russian Foundation for Basic Research (Grant Nos 12-02-31344, 12-02-33074 and 12-02-12101 ofi_m), the RF Ministry of Education and Science (Agreement Nos 8626, 14.132.21.1433 and 14.V37.21.0770) and the Presidium of the Russian Academy of Sciences (Extremely Strong Optical Fields and Their Applications Programme). E.A. Anashkina acknowledges the support from the Dynasty Nonprofit Foundation (Support Programme for Graduate Students and Young Pre-Degree Scientists).

References

1. Zinkstok R.T., Witte S., Hogervorst W., Eikema K.S.E. *Opt. Lett.*, **30**, 78 (2004).
2. Ishii N., Turi L., Yakovlev V.S., Fuji T., Krausz F., Baltuska A., Butkus R., Veitas G., Smilgevicius V., Danielius R., Piskarskas A. *Opt. Lett.*, **30**, 567 (2005).
3. Witte S., Zinkstok R.T., Hogervorst W., Eikema K.S.E. *Opt. Express*, **13**, 4903 (2005).
4. Lozhkarev V.V., Freidman G.I., Ginzburg V.N., Katin E.V., Khazanov E.A., Kirsanov A.V., Luchinin G.A., Mal'shakov A.N., Martyanov M.A., Palashov O.V., Poteomkin A.K., Sergeev A.M., Shaykin A.A., Yakovlev I.V. *Laser Phys. Lett.*, **4**, 421 (2007).
5. Rodwell M.J.W., Bloom D.M., Weingarten K.J. *IEEE J. Quantum Electron.*, **25**, 817 (1989).
6. Xu S., Zhai H., Wu K., Peng Y., Wu J., Zeng H. *Opt. Express*, **14**, 2487 (2006).
7. Andriukaitis G., Balčiūnas T., Ališauskas S., Pugžlys A., Baltuška A., Popmintchev T., Chen M.-C., Murnane M.M., Kapteyn H.C. *Opt. Lett.*, **36**, 2755 (2011).

8. Teisset C., Ishii N., Fuji T., Metzger T., Köhler S., Holzwarth R., Baltuška A., Zheltikov A., Krausz F. *Opt. Express*, **13**, 6550 (2005).
9. Andrianov A.V., Anashkina E.A., Muraviov S.V., Kim A.V. *Opt. Lett.*, **35**, 3805 (2010).
10. Anashkina E.A., Andrianov A.V., Muraviov S.V., Kim A.V. *Opt. Express*, **19**, 20141 (2011).
11. Okhotnikov O.G., Grudinin A.B., Pesa M. *New J. Phys.*, **6**, 177 (2004).
12. Ilday F., Buckley J., Kuznetsova L., Wise F. *Opt. Express*, **11**, 3550 (2003).
13. Fermann M., Galvanauskas A., Stock M., et al. *Opt. Lett.*, **24**, 1428 (1999).
14. Kieu K., Jones R., Peyghambarian N. *Opt. Express*, **18**, 21350 (2010).
15. Akhmediev N., Karlsson M. *Phys. Rev. A*, **51**, 2602 (1995).
16. Wai P.K.A., Chen H.H., Lee Y.C. *Phys. Rev. A*, **41**, 426 (1990).
17. Trebino R. *Frequency-resolved Optical Gating: the Measurement of Ultrashort Laser Pulses* (Boston: Kluwer Acad., 2000).
18. Husakou A.V., Herrmann J. *Phys. Rev. Lett.*, **87**, 203901 (2001).
19. Agrawal G.P. *Nonlinear Fiber Optics* (San Diego: Academic, 1995; Moscow: Mir, 1996).
20. Dudley J. *Rev. Mod. Phys*., **78**, 1135 (2006).
21. Lu F., Deng Y., Knox W.H. *Opt. Lett.*, **30**, 1566 (2005).
22. Chang G., Chen L.J., Kärtner F.X. *Opt. Express*, **19**, 6635 (2011).
23. Austin D., de Sterke C., Eggleton B., Brown T. *Opt. Express*, **14**, 11997 (2006).
24. Paschotta R., Nilsson J., Tropper A.C., Hanna D.C. *IEEE J. Quantum Electron.*, **33**, 1049 (1997).
25. Strickland D., Mourou G. *Opt. Commun.*, **56**, 219 (1985).